Hydrophilic/Hydrophobic Balance Determines Morphology of Glycolipids with Oligolactose Headgroups

Matthias F. Schneider,* Roman Zantl,* Christian Gege,† Richard R. Schmidt,† Michael Rappolt,‡ and Motomu Tanaka*

*Lehrstuhl für Biophysik E22, Technische Universität München, D-85748 Garching, Germany; †Fachbereich Chemie, Universität Konstanz, Fach M-725, D-78457 Konstanz, Germany; and ‡Institute of Biophysics and X-ray Structure Research, Austrian Academy of Sciences, Schmiedlstrasse 6, 8042 Graz, Austria

ABSTRACT The morphology of synthetic glycolipids with lactose oligomers (Lac *N*, the number of lactose units, $N = 1, 2, 3$) was studied in lamellar phase. By a systematic combination of differential scanning calorimetry and small- and wide-angle x-ray scattering experiments, the effects of hydrophilic/hydrophobic balance on their thermotropic phase behaviors were discussed. The dispersion of Lac 1 exhibited a crystalline-fluid phase transition, dominated by the strong van der Waals interaction between dihexadecyl chains. In the case of Lac 2, the hydrophilic/hydrophobic balance between the headgroup and the alkyl chains is shifted to the hydrophilic side, resulting in a gel-fluid phase transition with a decreased transition temperature and phase transition enthalpy. Different from the first two systems, the differential scanning calorimetry trace of Lac 3 showed much less remarkable peaks. The small- and wide-angle x-ray diffraction patterns did not reveal any transition in the chain ordering, suggesting that the correlation between the hexasaccharide headgroups is so strong that the melting of the alkyl chains was not allowed. Such dominant effects of the hydrophilic/hydrophobic balance on the morphology of Lac *N* lipids can be attributed to the small sterical mismatch between the alkyl chains and the linear, cylindrical oligolactose groups.

INTRODUCTION

Cell surface glycocalices play fundamental and essential roles in attenuating cell-cell and cell-matrix interaction. They serve not only as soft cushions between cells due to their unique swelling behaviors but also as specific recognition sites for counterpart lectins and cell adhesion receptors (Curatolo, 1987; Hakomori, 1990; Hakomori and Igarashi, 1995; Springer, 1995; Gabius and Gabius, 1997; Geyer et al., 2000). For example, blood group- and tumor-associated antigens such as sialyl Lewis^X and sialyl Lewis^A interact specifically with selectins (Crocker and Feizi, 1996; Varki, 1994; Vogel et al., 1998).

The previous studies on the extracted glycolipids from natural cells (Shipley et al., 1973; Sen et al., 1982) have been encountered by very complex interplay of different physical forces (entropic forces between branched saccharides, electrostatic interactions between charged groups, and mismatches in hydrophobic chains, etc.). To understand these intermolecular forces, many synthetic lipids have been proposed as artificial glycocalix models. Among various model systems, phospholipids with poly(ethylene glycol) chains have been widely applied in numerous fields (Harris, 1992). Effects of the ethyleneglycol chain on the phase behavior and the interface activity have been discussed using various methods (Kuhl et al., 1994, 1998; Kenworthy et al., 1995a, b; Naumann et al., 1999; Mathe et al., 2000). Morphology of synthetic glycolipids with mono- or disaccharide headgroups has intensively been studied (Sen et al., 1982; Mannock et al., 1994; Hinz et al., 1991). However, only several reports have been conducted on the glycolipids with linear oligosaccharide headgroups (Hinz et al., 1991; Hato and Minamikawa, 1996; Tamada et al., 1996; Köberl et al., 1998; Hato et al., 1999; Saxena et al., 2000).Recently, we reported the thermodynamic properties and swelling behavior of ether-linked glyco-glycerolipids with linear oligolactose headgroups (Schneider et al., 2001). We demonstrated that thermodynamic properties of the glycolipid monolayers at air/water interface are comparable to that of ordinary phospholipids, despite the lower degree of cooperativity between the larger headgroups. The swelling behavior of the transferred monolayer was quantitatively studied by ellipsometry under controlled humidity. For the lipids with lactose units of $N = 2$ and 3, the swelling curves could be fitted very well by those of polymer brushes, whereas the lipids with one lactose unit swelled like a ''rigid-rod''.

In this paper, we studied the morphology of lipids with lactose oligomers (the number of lactose units, $N = 1, 2, 3$) in the lamellar phase by differential scanning calorimetry (DSC) and small- and wide-angle x-ray scattering experiments (SAXS and WAXS). Effects of the hydrophilic/hydrophobic balance on their thermotropic phase behaviors were discussed systematically.

MATERIALS AND METHODS

The glycolipids were named Lac *N*, corresponding to the number of lactose units, $N = 1$, 2, and 3. As presented in Fig. 1, the lipids are ether-linked dihexadecyl glyco-glycerolipids. Details of the synthesis have been reported elsewhere (Schneider et al., 2001). For differential heat capacity (DSC) measurements, the glycolipids were dispersed in ultra-pure water (Millipore, Molsheim, France) by freeze-thawing. DSC scans of the glycolipid

Submitted July 23, 2001, and accepted for publication August 28, 2002.

Address reprint requests to Motomu Tanaka, Lehrstuhl für Biophysik E22, Technische Universität München, D-85748 Garching, Germany. Fax: 49-89-289-12469; E-mail: mtanaka@ph.tum.de.

0006-3495/03/01/306/08 $2.00

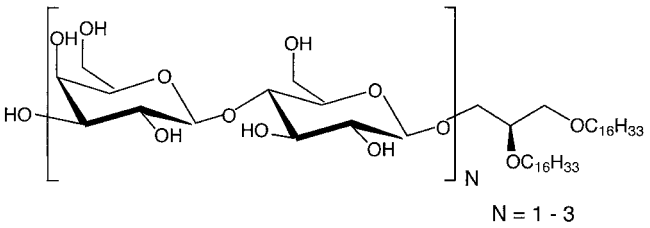

FIGURE 1 Chemical structures of the glycolipids with oligolactose headgroups, Lac N ($N = 1$–3).

dispersions (1 mg/mL) were recorded with a Microcal VP-DSC Micro Calorimeter (Microcal Software, Northampton, MA) at the heating rate of 15°C/h. Before the measurements, one heating/cooling cycle between 5°C and 90°C was applied to compensate the thermal history. To confirm the equilibration, several heating/cooling cycles were repeated. For each cycle, the temperature was held for 20 min at 5°C and 5 min at 90°C, respectively. Measured data were analyzed using the routines of the Origin software (Microcal). For x-ray scattering experiments, the glycolipid suspensions with the concentration of 20 wt % were filled into quartz capillaries (Hilgenberg, Malsfeld, Germany). The samples in the capillaries were centrifuged and flame-sealed. X-ray measurements have been performed after repeating several heating/cooling cycles. SAXS data were measured at the synchrotron beamline ID2A of the European Synchrotron Radiation Facility (ESRF, Grenoble), with a resolution better than $\Delta q = 0.0015$ Å^{-1}. WAXS data were taken at the beamline D43 of Laboratoire pour l'Utilisation du Rayonnement Electromagnétique (LURE, Paris). In this case the resolution was $\Delta q = 0.0055$ Å^{-1}. In both cases, SAXS and WAXS, the observation of isotropic Debye-Scherrer rings indicated that all the samples consisted of perfect powders. The reproducibility of the measurements has also been checked by preparing the samples with different concentration (50 wt %, measured at LURE). The radial integration of the two-dimensional data recorded using the local CCD camera at ID2A was carried out by the standard routines of ESRF. At LURE, data were collected using Fuji image plates in combination with homemade data processing software on the basis of IGOR Pro (Wave Metrics, USA). The effects of the broad and weak DSC peaks were further studied by another series of SAXS and WAXS measurements under more careful temperature scans at the beamline A2 of Hamburger Synchrotronstrahlungslabor (HASY LAB, Hamburg). The homemade program processed the results gained from the linear detector.

RESULTS

All the measured DSC data (transition temperature and enthalpy) and the diffraction peaks obtained by SAXS and WAXS experiments are summarized in Table 1, and the details are described for each lipid in the following subsections.

Crystalline-fluid phase transition of Lac 1

The heat capacity trace of Lac 1 is given in Fig. 2 *a*, exhibiting a sharp transition at $T_t = 74$°C and the phase transition enthalpy of $\Delta H = 30$ kcal/mol. A distinct and broad enthalpic peak was also observed at around $T_p = 60$°C. As can be seen in Fig. 2 *a*, we observed no hysteresis within the second, third, and fourth heating. The DSC traces were entirely reproducible. In contrast to the previous work on similar C16:0-lactosyl-ceramide (Saxena et al., 2000), our results did not exhibit any evidence for a metastable phase at low temperature. In fact, all the measurements were carried out at a very slow heating/cooling rate (15°C/h), which was ~6–20 times slower than that used in the reference.

TABLE 1 The measured phase transition temperatures (T_t / T_p), phase transition enthalpy (ΔH), and low- and wide-angle spacings (d_{SAXS} and d_{WAXS})

			Lac 1	Lac 2	Lac 3
		T_t / T_p [°C]	74/60	50/40	—*
DSC		ΔH [kcal/mol]	30	9.2	—
Phase	L_C/L_C'	d_{SAXS} [Å]	68	—	108
		d_{WAXS} [Å]	3.76, 4.45, 7.50†	—	4.19, 4.46, 7.61†
	L_β	d_{SAXS} [Å]	—	87	—
		d_{WAXS} [Å]	—	4.17	—
	L_α	d_{SAXS} [Å]	60	78	—
		d_{WAXS} [Å]	4.57	4.45	—

*No phase transition was observed until $T = 80$°C.
†The diffraction peaks corresponding to the headgroup correlation.

The powder-averaged small-angle x-ray scattering data at $T = 20$, 40, 60, and 80°C are summarized in Fig. 2 *b* (*left*), indicating periodic three-dimensional lamellar structures. Across the transition at $T_t = 74$°C, the periodicity of the low-angle spacing was changed from 68 Å (*below*) to 60 Å (*above*), suggesting the ''melting'' of the dihexadecyl chains. In fact, SAXS measurements at LURE for the samples with a different concentration (50 wt %) also confirmed that there is no thermal hysteresis. As shown in Fig. 2 *b* (*right*), the wide-angle patterns at $T < T_t$ ($T = 20$°C) can be characterized with three pronounced scatterings at 3.76, 4.45, and 7.50 Å. The scattering peak at 4.45 Å corresponds to the alkyl chains in the lamellar crystalline (L_C) phase with a triclinic packing mode (Larrson, 1988). On the other hand, the peak at 7.50 Å can be interpreted as the first order peak due to the strong correlation between dehydrated headgroups (Caffrey, 1987; Hinz et al., 1991; Köberl et al., 1998; Seddon et al., 1984). The other peak at 3.76 Å can be related either to 1), the complex chain packing modes, e.g., the hybrid lattice of orthorhombic and triclinic (Köberl et al., 1998; Saxena et al., 2000), or to 2), the second order peak of the headgroup correlation peak at 7.50 Å. Interestingly, both the lamellar distance (Fig. 2 *b*, *left*) and the WAXS peak showed no changes across $T_p = 60$°C, where the broad enthalpic peak was observed by DSC, in comparison to those at 20°C (Table 2, *top*). At $T > T_t$ ($T = 80$°C), a broad band at ~4.57 Å could be observed, suggesting the fluid L_α phase of the alkyl chains. Furthermore, the scattering peaks from the headgroup correlation disappeared because the lactose groups were hydrated. Thus it has been demonstrated that the Lac 1 lamellar has a direct transition from the crystalline L_C phase to the fluid L_α phase.

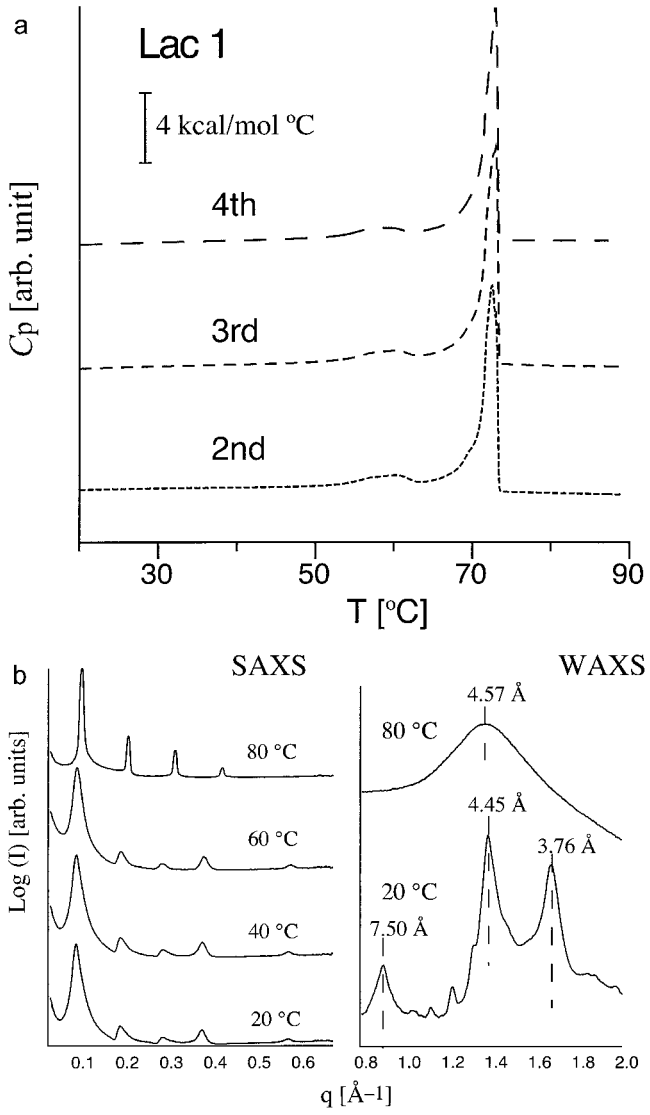

FIGURE 2 (a) Differential heat capacity scans of the Lac 1 dispersion (1 mg/mL) recorded at the heating rate of 10°C/h, exhibiting a sharp transition at $T_t = 74$°C and the phase transition enthalpy of $\Delta H = 30$ kcal/mol. A distinct and broad enthalpic peak was also observed at around $T = 60$°C. The successive heating scans showed no hysteresis. (*b*) Powder-averaged small-angle x-ray scattering (SAXS) data of the lamellar dispersion of Lac 1 at $T = 20$, 40, 60, and 80°C (*left*). The lamellar spacing showed a transition between 60°C ($d_{SAXS} = 68$ Å) and 80°C ($d_{SAXS} = 60$ Å). Wide-angle x-ray scattering (WAXS) data suggested the transition between the crystalline L_C phase and the fluid L_α phase (*right*).

Gel-fluid phase transition of Lac 2

Fig. 3 *a* shows the DSC scan of Lac 2. Compared to that of Lac 1, the main transition peak was broadened and the T_t was reduced to $T_t = 50$°C. The phase transition enthalpy was also clearly reduced to $\Delta H = 9.2$ kcal/mol. A broad enthalpic peak was still observed at around $T_p = 40$°C. The small-angle x-ray scattering data at $T = 20$, 40, 60, and 80°C (Fig. 3 *b*, *left*) showed periodic lamellar structures. Across $T_t = 50$°C, the low-angle spacing was changed from 87 Å at $T <$

TABLE 2 Correlation distance of Lac 1 (*top*) and Lac 2 (*middle*) lamellar at the "intermediate" phase (between weak transition peak and main peak), obtained by SAXS and WAXS measurements at another beamline (HASY LAB, A2)

Lac 1	d_{SAXS} [Å]	d_{WAXS} [Å]
20°C	67	4.5, 3.8
65°C	67	4.5, 3.9
80°C	60	—
Lac 2	d_{SAXS} [Å]	d_{WAXS} [Å]
20°C	87	4.2
45°C	87	4.2
80°C	78	—
Lac 3	d_{SAXS} [Å]	d_{WAXS} [Å]
20°C	111	4.5, 4.2
45°C	111	4.5, 4.2
80°C	111	4.5, 4.2

For comparison, the corresponding results at the low temperature phase (L_C for Lac 1 and L_β for Lac 2, respectively) and L_α phases are also presented. The weak endothermic peak in DSC traces (60°C for Lac 1 and 40°C for Lac 2) resulted in no changes in chain ordering or lamellar distance. Furthermore, the broad DSC peaks observed for Lac 3 ($T = 25$, 55°C) lamellar do not correspond to changes in chain ordering or lamellar distance (*bottom*).

T_t to 78 Å at $T > T_t$, respectively. The reproducibility of the data was also checked by the SAXS measurement of a different sample (50 wt %) at LURE. Here, the wide-angle patterns at $T < T_t$ ($T = 20$°C) can be characterized with only one sharp scattering peak at 4.17 Å, which corresponds to the gel (L_β) phase. The absence of a pronounced shoulder denotes that the alkyl chains have nearly no tilts (Hinz et al., 1991; Köberl et al., 1998). No correlation between the lactose headgroups could be seen, indicating that the headgroups are already hydrated in this phase. At $T > T_t$ ($T = 80$°C), a broad band at ~4.45 Å could be observed, which is consistent with the fluid L_α phase without any headgroup correlation. The number of the equidistanced peaks in the small-angle scattering was smaller at $T > T_t$. Here we conclude that the Lac 2 lamellar has a transition between the gel phase and the fluid L_α phase. Furthermore, as presented in Table 2 (*middle*), the broad enthalpic peak at $T_p = 40$°C does not correspond to any changes in lamellar spacing or chain packing.

Crystalline mono phase of Lac 3

In contrast to Lac 1 and Lac 2, the phase behavior was significantly changed when the number of lactose units became $N = 3$. The DSC traces (Fig. 4 *a*) showed much less remarkable peaks until $T = 80$°C, the highest operating temperature for aqueous dispersion. The SAXS data (Fig. 4 *b*, *left*) exhibited more than 10 equidistanced peaks, suggesting a highly ordered lamellar structure. The low-angle spacing kept constant between 20°C and 80°C, 108 Å.

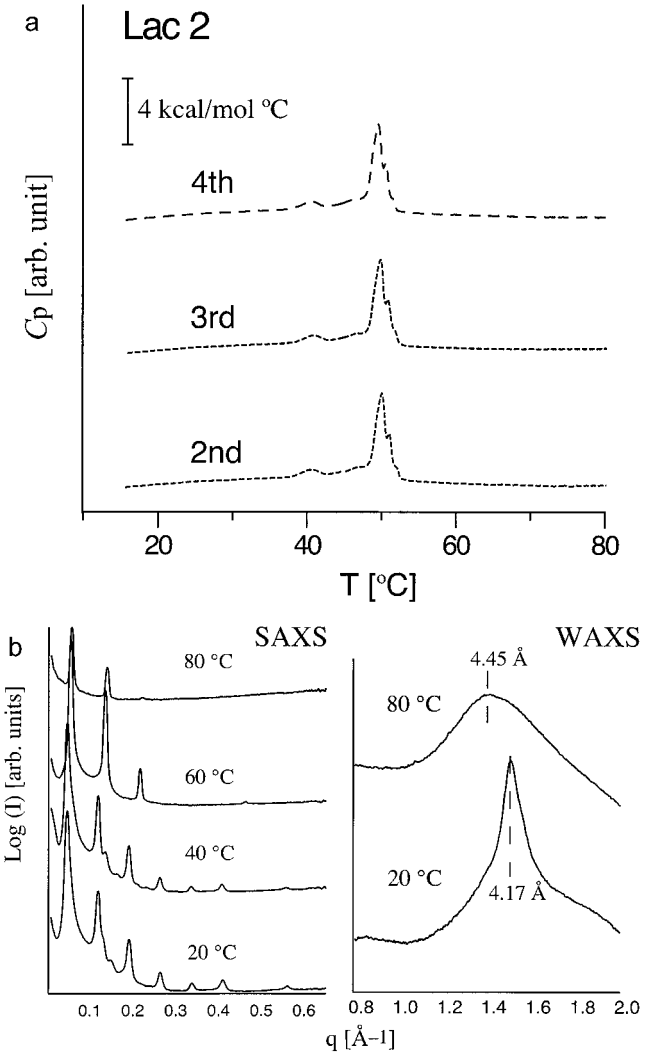

FIGURE 3 (*a*) Heat capacity traces of the Lac 2 dispersion (1 mg/mL), showing a broadened transition peak at $T_t = 50°C$ and another enthalpic transition at around $T = 40°C$. The phase transition enthalpy was also clearly reduced to $\Delta H = 9.2$ kcal/mol. No thermal hysteresis was observed within the subsequent heating scans. (*b*) SAXS diffraction patterns of the lamellar dispersion of Lac 2 at $T = 20$, 40, 60, and 80°C (*left*). The lamellar spacing showed a transition between 40°C ($d_{SAXS} = 87$ Å) and 60°C ($d_{SAXS} = 78$ Å). WAXS peaks suggested the transition between the gel phase and the fluid phase (*right*).

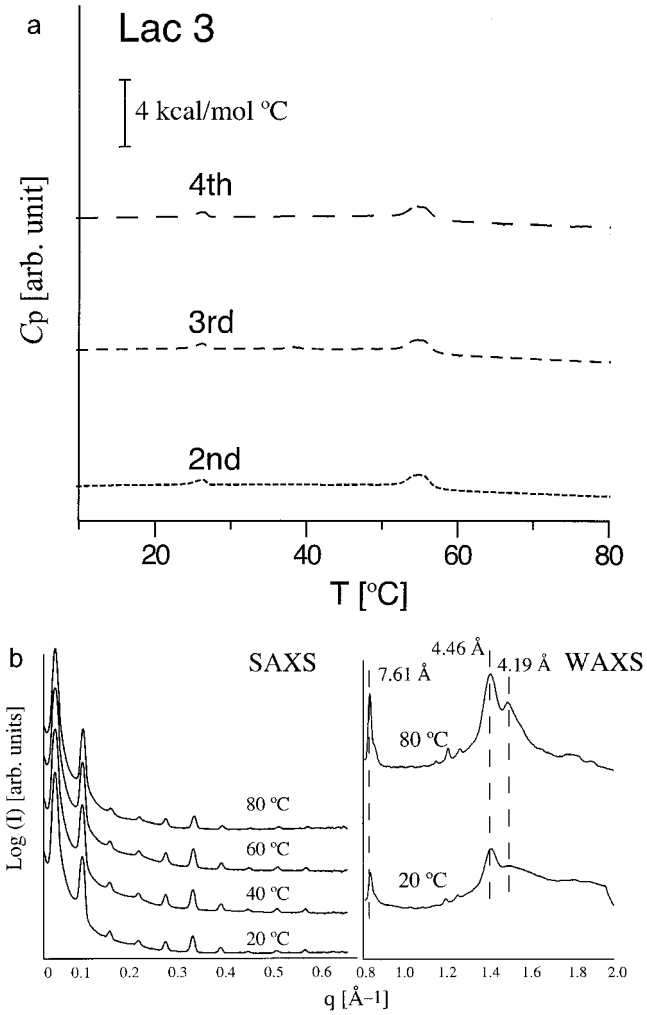

FIGURE 4 (*a*) DSC traces of the Lac 3 dispersion (1 mg/mL), showing no evidential endothermic peaks. The heat scans were entirely reproducible within the second (*bottom*), third (*middle*), and the fourth (*top*) scans. (*b*) SAXS diffraction patterns of the Lac 3 lamellar dispersion at $T = 20$, 40, 60, and 80°C (*left*). The lamellar spacing showed no transition at all measurement conditions, $d_{SAXS} = 108$ Å. WAXS peaks suggested that the Lac 3 lamellar takes crystalline-like phase, and no chain melting takes place (*right*).

For the sample with a concentration of 50 wt %, the SAXS data measured at LURE confirmed the reproducibility. The wide-angle scattering patterns (Fig. 4 *b*, *right*) suggested no transition, exhibiting three sharp scattering peaks at 4.19, 4.46, and 7.61 Å. The results clearly indicate that the Lac 3 lamellar has no chain melting. The sharp peak at 7.61 Å can be attributed to the strong headgroup correlation between the dehydrated headgroups. Judging from the peaks at 4.19 and 4.46 Å, dihexadecyl chains of Lac 3 take a highly packed crystalline-like phase with a slight tilt or defects. Moreover, it is also confirmed that the very weak enthalpic peaks around 25°C and 55°C do not induce any morphological transition (Table 2, *bottom*).

DISCUSSION

Thickness of each sublayer

The lamellar distance d_0 measured by SAXS can be represented by

$$d_0 = 2d_{ml} + d_w = 2(d_{al} + d_h) + d_w. \quad (1)$$

d_{ml} is the thickness of a lipid monolayer, consisting of the thickness of alkyl chains d_{al} and that of headgroups d_h. d_w stands for the thickness of the water layer between two

bilayers. For the crystalline phase of Lac 1 and Lac 3, the strong headgroup correlation denotes that there is no bulk water between the lamellar stacks (Seddon et al., 1984; Caffrey, 1985; Köberl et al., 1998). Because the wide-angle scattering also suggested that the tilt angle of the chains is almost negligible, the lamellar distance values obtained by SAXS, $d_{0(\text{Lac 1})} = 68$ Å and $d_{0(\text{Lac 3})} = 108$ Å are almost equal to the thickness of a single bilayer, $d_0 \approx 2d_{\text{ml}} = 2(d_{\text{al}} + d_{\text{h}})$. The WAXS peak of the Lac 2 in the gel phase indicates that the tilting of the alkyl chains is also very small and the headgroups are hydrated. Although the water layer thickness between the bilayers could not be determined experimentally, the lamellar distance value of Lac 2 ($d_{0(\text{Lac 2})} = 87$ Å) is exactly in the middle of $d_{0(\text{Lac 1})}$ and $d_{0(\text{Lac 3})}$.

If the oligolactose headgroups take linear, cylindrical conformation, the apparent thickness difference corresponding to one lactose unit, $\Delta d_{\text{h}} = 10$ Å, is very reasonable from the rough estimation of the monosaccharide size (~5 Å). Actually, our previous study on monolayers at air/water interface demonstrated that the area per Lac N molecule A in the liquid condensed phase (at $\pi \geq 25$ mN/m) is independent from the lactose unit number N: $A = 37-40$ Å^2 (Schneider et al., 2001). Other recent studies by NMR and molecular dynamic simulation have also shown that the tetrasaccharide lacto-*N*-neotetraose (similar to Lac 2 headgroup) takes uniaxial, cylindrical conformation in dilute liquid crystalline media such as phospholipid dispersions (Landersjö et al., 2000; Rundlöf et al., 1998).

Area per molecule

In the gel phase, the area per glycolipid molecule A can be determined by the wide-angle diffraction line w (Jähnig et al., 1979; Seddon et al., 1984)

$$\mathrm{A} = \frac{4}{\sqrt{3}}\mathrm{w}^2. \tag{2}$$

From the wide-angle spacing of Lac 2 in the L_β phase, $w_{L\beta(\text{Lac 2})} = 4.17$ Å, one can calculate the area per molecule, $A_{L\beta(\text{Lac 2})} = 40.2$ Å^2. This value shows good agreement with the area per molecule of the Lac N monolayer in the liquid condensed phase, $A = 37 \sim 40$ Å^2 (Schneider et al., 2001). On the other hand, the WAXS peaks in the fluid phase yielded apparently smaller values ($46 \sim 48$ Å^2) than those of fluid phospholipids, $A_{L\alpha} > 55$ Å^2 (Seddon et al., 1984; Sackmann, 1995). Indeed, McIntosh and Simon (1986) have demonstrated that the specific volume of the lipid and its changes due to the phase transition should be taken into account for the quantitative measure. Although such a simplification is not applicable to the crystalline L_C phase, the values obtained by monolayer experiments ($37 \sim 40$ Å^2) are still in good agreement with the minimum area $A = 36.5$ Å^2, which is the double of the area per single, crystalline alkane: 18.23 Å^2 (Nyburg and Lüth, 1972). This is another indirect evidence for the cylindrical structures of the Lac N lipids.

Effects of hydrophilic/hydrophobic balance on morphology

The lamellar dispersion of Lac 1 exhibited the transition between the crystalline L_C phase and the fluid L_α phase. Thermotropic phase transition temperature of the Lac 1 dispersion ($T_t = 74$°C) is apparently higher than that of other lipids with dihexadecyl chains, such as DPPC, $T_m = 41.4$°C, and the obtained transition enthalpy ($\Delta H = 30$ kcal/mol) is larger in comparison to the sum of transition enthalpies of DPPC from L_C phase to L_α phase (i.e., $L_C \rightarrow L_{\beta'} \rightarrow P_{\beta'} \rightarrow L_\alpha$), $\Delta H = 15$ kcal/mol (Cevc, 1993), respectively. Alkyl chains of Lac 1 are strongly correlated by the very strong van der Waals interaction, which even enabled them to form crystalline-like tight packing with almost no tilting. The additional enthalpic contribution can be due to the hydrogen bonding between the Lac 1 headgroups that are free from dipoles, in contrast to phospholipids with P–N dipoles (Cevc, 1993). Nevertheless, further structural characterizations are necessary to understand the small satellite peaks observed in the L_C phase, which indicate in-plane correlations.

When an additional lactose group was attached to the headgroup, the hydrophilic/hydrophobic balance between the headgroup and the alkyl chains is shifted to the hydrophilic side. This shift in the balance reduces the cooperativity between the alkyl chains, resulting in the decrease in the transition temperature and the phase transition enthalpy. The strongly crystallized alkyl chain packing was modulated to the gel phase, which allows the hydration of the headgroups.

The change in the Gibbs free energy between two phases can be expressed as

$$\Delta\mathrm{G} = \Delta\mathrm{H} - \mathrm{T}\Delta\mathrm{S}. \tag{3}$$

At the phase transition temperature T_t, $\Delta G = 0$ and therefore,

$$\Delta\mathrm{S} = \Delta\mathrm{H}/\mathrm{T_t}. \tag{4}$$

As the transition enthalpy and temperature could be measured experimentally, the entropy can be calculated by Eq. 4. This leads to a change in phase transition entropy:

$$\Delta(\Delta\mathrm{S}) = \Delta\mathrm{S}_{(\text{Lac2})} - \Delta\mathrm{S}_{(\text{Lac1})} = -59\,\mathrm{kcal/mol} * \mathrm{K}. \tag{5}$$

The decrease in transition entropy from Lac 1 to Lac 2 agreed well with the morphology suggested by x-ray diffraction. Below the phase transition temperature, Lac 1 is in the highly ordered crystalline L_C phase, whereas Lac 2 takes the gel (L_β) phase due to the hydration of the headgroups. Thus, the higher degree of order in the crystalline phase can be related directly to the difference in the phase transition entropy.

Totally different from the first two systems, the DSC trace of Lac 3 did not have remarkable endothermic peaks. The WAXS data did not reveal any transition in the chain ordering, exhibiting two sharp scattering peaks due to the slightly tilted alkyl chains and one sharp correlation peak due to the headgroups. The small-angle scattering also

demonstrated the highly ordered three-dimensional lamellar structure with more than 10 sharp diffraction peaks with a constant distance, 108 Å. In this case, the very strong correlation between the hexasaccharide headgroups forced the alkyl chain to take the tight, crystalline-like packing, which is different from the ideal hexagonal lattice. Because the attractive interaction between the headgroups is so strong, the hydration does not take place any longer.

Such hydrophobic appearance of linear oligo- and polysaccharides has been well known for cellooligosaccharides and cellulose. For example, Sano et al. had reported that cellooligosaccharides are monomolecularly soluble in water when the monosaccharide unit number was $N = 1 \sim 4$, although it can be dissolved only in an aggregate state when $N = 5$ (Sano et al., 1991). Hato et al. had reported a similar phase for the lipid with two dodecanoyl chains and cellooligosaccharides with $N = 5$, which they named ''a hydrated crystal'' (Hato and Minamikawa, 1996; Hato et al., 1999). But, the interpretation of this phase behavior seemed still difficult. Indeed, cellulose is insoluble in most of the solvents as well as in water (Brandrup and Immergut, 1975). Recently, we found that the water uptake ability of the highly ordered cellulose films is obviously poorer (Rehfeldt and Tanaka, unpublished results) compared to that of dextran films (Mathe et al., 1999).

We tentatively understand this L_C' phase of Lac 3 in terms of a ''frozen'' bilayer, which can appear either at very low temperature conditions or at very high surface pressures (Sackmann, 1995; Lipowsky, 1991). The WAXS peak positions can be related to the chain tilting, in-plane defects, or the buckling induced by the strong headgroup correlation. To gain more insight in the structural characteristics of this phase, further conformational analysis by spectroscopic techniques such as FTIR and the systematic link to the morphology in two dimensions, i.e. morphology of monolayers, must be performed.

Electron density profiles of some representative phases

Structural analyses of several representative phases were attempted by reconstruction of the electron density profiles (Harper et al., 2001). The measured SAXS data were fitted with Gaussians after subtraction of background scattering. A Lorentz correction was applied by multiplying each peak intensity (peak area) by its corresponding wave vector q (Warren, 1969). The square root of the corrected peak intensity was finally used to determine the constant form factor F of each respective reflection. The electron density profile relative to the constant electron density profile of water was calculated by the Fourier synthesis

$$\tilde{\rho}(z) = \sum_{h=1}^{h\,max} \pm F_h \cos\left(\frac{2\pi h z}{d}\right), \qquad (6)$$

where h is the order of reflection and d the lamellar spacing. For centrosymmetric crystals such as lamellar stacks of lipid bilayers, the electron density can be presented as a Fourier series of cosines, therefore, the unknown phases are either 0° (+) or 180° (−). In the following consideration, the origin was set to the center of the methyl dip by fixing the phase of the first order reflection to ''−''. All peak-fittings and further calculations were carried out with the software package Origin 5.0 (Microcal).

First, the SAXS data of Lac 1 at 80°C and Lac 2 at 60°C (L_α phase) were analyzed. Each, four strong reflections $h =$ 1, 2, 3, 4 of Lac 1 and $h = 1, 2, 3, 6$ of Lac 2 were considered for the Fourier synthesis. Out of the possible $2^4 = 16$ combinations, we chose eight combinations that are centered in the middle of the bilayers ''− − − −, − − − +, − − + −, − − + +, − + − −, − + − +, − + + −, − + + +'', corresponding to the terminal methyl dip (−). The most plausible phasing ''− − + −'' shows a good similarity in the hydrocarbon chains region to the very well studied L_α phase of dipalmitoylphosphatidylethanolamine (Pabst et al., 2000), and displays the appropriate headgroup size: ~10 Å for Lac 1 and 20 Å for Lac 2, respectively. All the other phase combinations lead to inappropriate structural features, such as too big hydrocarbon core, missing methyl dip, or too small headgroup size. By assuming that the maximum of each electron density profile in Fig. 5 *a* displays the midpoint of headgroups, thickness of the alkyl chains d_{al} can be estimated to be 15–17 Å for both Lac 1 and Lac 2. This is in good agreement with the corresponding value reported for dipalmitoylphosphatidylethanolamine of, at 74°C, 15.4 Å. From the obtained d_{al} value, the thickness of the water layer between two bilayers was calculated to be 6–8 Å.

SAXS diffraction pattern of the crystalline-like phase of Lac 3 (at 20°C) displays 10 diffraction orders (Fig. 4 *b*), which results in $2^9 = 512$ different possible phase combinations. The simple approach to choose the most reasonable matching from all possible results obviously fails in this case. Therefore, we have developed a simple three-strip model for the L_c phase of Lac 3 (Fig. 5 *b*, *bottom*), based on the lactose headgroup, the hydrocarbon, and the mid-plane region. Here, the water layer was not taken into account because strong headgroup correlation in the crystalline phase of Lac 1 and Lac 3 suggested that there should be no bulk water between the bilayers. The electron density of the headgroup was estimated from the density of lactose of 1.525 g/cm^3 and its molar mass of 342.0 g to be ~0.48 e/Å^3. The electron density of the hydrocarbon region, 0.30 e/Å^3, and the terminal methyls, of 0.16 e/Å^3, were taken from the work of Harper et al. (2001). Width of the headgroup region was set to 30 Å by assuming a cylindrical conformation, whereas that of the methyl trough was assumed to be 8 Å (Wiener et al., 1989). The phasing that results in the electron density plot with the smallest mean absolute deviation to the simple three-strip model is given in Table 3. The final electron density profile is superimposed to

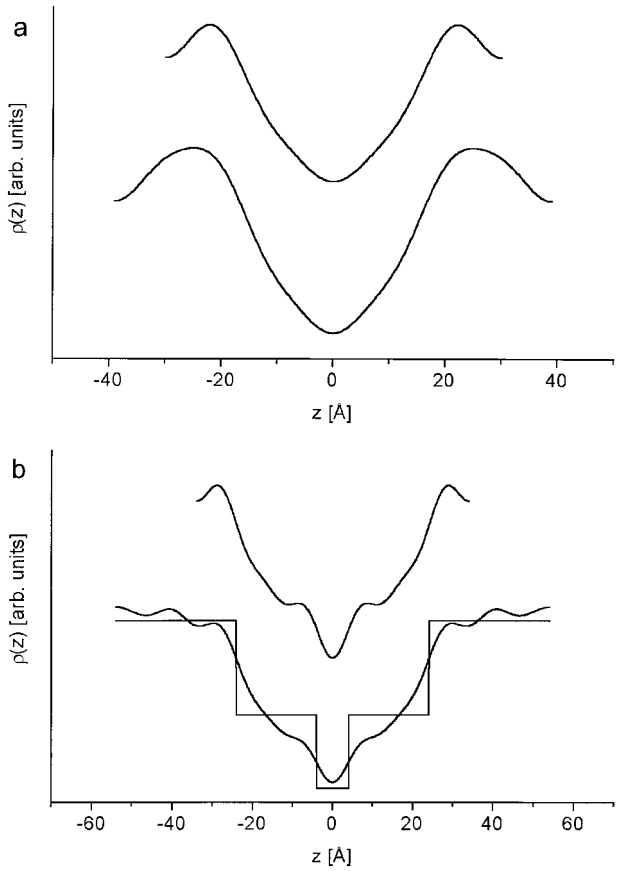

FIGURE 5 (*a*) Electron density profiles calculated from SAXS diffraction patterns of Lac 1 at 80°C (top), and that of Lac 2 at 60°C (*bottom*). Under these conditions, the glycolipids are in fluid L_α phase. (*b*) Electron density profile of crystalline-like Lac 1 at 20°C calculated from $h = 1, 2, 3, 4, 6$ (*top*) and that of Lac 3 at 20°C obtained from a simple three-strip model (*bottom*).

the model (Fig. 5 *b*, *bottom*). It is noteworthy that the given resolution enables one to distinguish each lactose unit at the positions of $\sim z = \pm 29$, ± 40, and ± 52 Å.

SAXS data of Lac 1 at 20°C, corresponding to crystalline phase, was analyzed by taking the reflections $h = 1, 2, 3, 4, 6$ into account. Among the 16 possible solutions, four reasonable candidates were found "$- - - - -$, $- + - - -$, $- - + - -$, $- + + - -$" to be consistent with typical lipid bilayer features. Here, we chose "$- + - - -$" as the final solution (Fig. 5 *b*, *top*) because the corresponding electron density profile shows the best similarity in the hydrocarbon chains region with that of Lac 3 at 20°C. The headgroup center at $z = \pm 29$ Å almost coincides with the first lactose position of Lac 3, and the alkyl chain length d_{al} is $\sim$24 Å in both crystalline phases.

Here we refrained from determining the electron density profile of Lac 2 at 20°C (gel phase), because the subpeak between the $h = 2$ and 3 could not be explained.

The authors are most indebted to Prof. E. Sackmann for his constant support and helpful suggestions throughout this work. We appreciate Drs. F. Artzner and S. S. Funari for the assistance in SAXS and WAXS experiments at LURE/ESRF and HASY LAB, respectively, as well as for their constructive comments.

This work was supported by the Deutsche Forschungs Gemeinschaft (DFG Sa 246/30, Schm 213/36), and by the Fonds der Chemischen Industrie. M.T. is grateful to Alexander von Humboldt-Stiftung for the postdoctoral fellowship and DFG for the Habilitation fellowship (Emmy Noether Program, Ta 259/1).

TABLE 3 Summary of the Fourier coefficients F_h, which have been used to determine the electron density maps of Fig. 5

h	F_h (Lac 1 at 80°C)	F_h (Lac 2 at 60°C)	F_h (Lac 1 at 20°C)	F_h (Lac 3 at 20°C)
1	−1	−1	−1	−1
2	+0.22	+0.58	+0.11	−0.28
3	−0.18	−0.15	−0.07	−0.03
4	−0.10	—	−0.17	+0.04
5	—	—	—	−0.05
6	—	−0.04	−0.10	−0.08
7	—	—	—	−0.05
8	—	—	—	+0.03
9	—	—	—	−0.04
10	—	—	—	−0.03

Note that the amplitudes have been normalized to the first order amplitudes and there phases were set "−", so that the mid-plane of the bilayer coincides with the origin.

REFERENCES

Brandrup, J., and E. H. Immergut. 1975. Polymer Handbook. Wiley Interscience, New York.

Caffrey, M. 1985. Kinetics and mechanism of transitions involving the lamellar, cubic inverted hexagonal and fluid isotropic phases of hydrated monoacylglycerides monitored by time-resolved X-ray diffraction. *Biochemistry*. 26:6349–6363.

Caffrey, M. 1987. Kinetics and mechanism of transitions involving the lamellar, cubic, inverted hexagonal, and fluid isotropic phases of hydrated monoacylglycerides monitored by time-resolved X-ray diffraction. *Biochemistry*. 26:6349–6363.

Cevc, G. 1993. Phospholipids Handbook. Marcel Dekker, New York.

Crocker, P. R., and T. Feizi. 1996. Carbohydrate recognition systems: functional triads in cell-cell interactions. *Curr. Opin. Struct. Biol.* 6:679–691.

Curatolo, W. 1987. Glycolipid function. *Biochim. Biophys. Acta*. 906: 137–160.

Gabius, H. J., and S. Gabius. 1997. Glycoscience. Chapmann & Hall, Weinheim, Germany.

Geyer, A., C. Gege, and R. R. Schmidt. 2000. Calcium-dependent carbohydrate-carbohydrate recognition between Lewis X blood group antigens. *Angew. Chem. Int. Ed.* 39:3245–3249.

Hakomori, S. 1990. Bifunctional role of glycosphingolipids. Modulators for transmembrane signaling and mediators for cellular interactions. *J. Biol. Chem.* 265:18713–18716.

Hakomori, S., and Y. Igarashi. 1995. Functional role of glycosphingolipids in cell recognition and signaling. *J. Biochem.* 118:1091–1103.

Harper, P. E., D. A. Mannock, R. N. A. H. Lewis, R. N. McElhaney, and A. M. Gruner. 2001. X-ray diffraction structures of some phosphatidylethanolamine lamellar and inverted hexagonal phases. *Biophys. J.* 81: 2693–2706.

Harris, J. M. 1992. Poly(ethylene glycol) Chemistry. Plenum Press, New York.

Hato, M., and H. Minamikawa. 1996. The effects of oligosaccharide stereochemistry on the physical properties of aqueous synthetic glycolipids. *Langmuir*. 12:1658–1665.

Hato, M., H. Minamikawa, K. Tamada, T. Baba, and Y. Tanabe. 1999. Self-assembly of synthetic glycolipid/water systems. *Adv. Coll. Interf. Sci.* 80:233–270.

Hinz, H. J., H. Kuttenreich, R. Meyer, M. Renner, R. Fründ, R. Koynova, A. I. Boyanov, and B. G. Tenchov. 1991. Stereochemistry and size of sugar head groups determine structure and phase behavior of glycolipid membranes: densiometric, calorimetric, and X-ray studies. *Biochemistry*. 30:5125–5138.

Jähnig, F., K. Harlos, H. Vogel, and H. Eibl. 1979. Electrostatic interactions at charged lipid membranes. Electrostatically induced tilt. *Biochemistry*. 18:1459–1468.

Kenworthy, A. K., K. Hristova, D. Needham, and T. J. McIntosh. 1995a. Range and magnitude of the steric pressure between bilayers containing phospholipids with covalently attached poly(ethylene glycol). *Biophys. J.* 68:1921–1936.

Kenworthy, A. K., S. A. Simon, and T. J. McIntosh. 1995b. Structure and phase behavior of lipid suspensions containing phospholipids with covalently attached poly(ethylene glycol). *Biophys. J.* 68:1903–1920.

Köberl, M., H. J. Hinz, and G. Rapp. 1998. Temperature scanning simultaneous small- and wide-angle X-ray scattering studies of glycolipid vesicles: areas, expansion coefficients and hydration. *Chem. Phys. Lipids.* 91:13–37.

Kuhl, T. L., D. E. Leckband, D. D. Lasic, and J. N. Israelachvili. 1994. Modulation of interaction forces between bilayers exposing short-chained ethylene oxide headgroups. *Biophys. J.* 66:1479–1488.

Kuhl, T. L., J. Majewski, J. Y. Wong, S. Steinberg, D. E. Leckband, J. N. Israelachvili, and G. S. Smith. 1998. A neutron reflectivity study of polymer-modified phospholipid monolayers at the solid-solution interface: polyethylene glycol-lipids on silane-modified substrates. *Biophys. J.* 75:2352–2362.

Landersjö, C., C. Höög, A. Maliniak, and G. Widmalm. 2000. NMR investigation of a tetrasaccharide using residual dipolar couplings in dilute liquid crystalline media: Effect of the environment. *J. Phys. Chem. B.* 104:5618–5624.

Larrson, K. 1986. Physical properties—structural and physical characteristics. *In* The Lipid Handbook. F. D. Gunstone, J. L. Harwood, and F. B. Padley, editors. Chapman and Hall, London. 321–337.

Lipowsky, R. 1991. The conformation of membranes. *Nature*. 349:475–481.

Mannock, D. A., R. N. McElhaney, P. E. Harper, and S. M. Gruner. 1994. Differential scanning calorimetry and X-ray diffraction studies of the thermotropic phase behavior of the diastereomeric di-tetradecyl-beta-D-galactosylglycerols and their mixture. *Biophys. J.* 66:734–740.

Mathe, G., A. Albersdörfer, K. R. Neumaier, and E. Sackmann. 1999. Disjoining pressure and swelling dynamics of thin adsorbed polymer films under controlled hydration conditions. *Langmuir*. 15:8726–8735.

Mathe, G., C. Gege, K. R. Neumaier, R. R. Schmidt, and E. Sackmann. 2000. Equilibrium swelling behavior of solid supported poly(ethylene glycol) lipid monolayers. Effects of short chain lengths. *Langmuir*. 16:3835–3845.

McIntosh, T. J., and S. A. Simon. 1986. Area per molecule and distribution of water in fully hydrated dilauroylphosphatidylethanolamine bilayers. *Biochemistry*. 25:4948–4952.

Naumann, C. A., C. F. Brooks, G. G. Fuller, W. Knoll, and C. W. Frank. 1999. Viscoelastic properties of lipopolymers at the air-water interface: A combined interfacial stress rheometer and film balance study. *Langmuir*. 15:7752–7761.

Nyburg, S. C., and H. Lüth. 1972. n-Octadecane: A correction and refinement of the structure given by Hayashida. *Acta Crystallogr*. B28: 2992–2995.

Pabst, G., M. Rappolt, H. Amenitsch, and P. Laggner. 2000. Structural information from multilamellar liposomes at full hydration: Full q-range fitting with high quality x-ray data. *Phys. Rev. E.* 62:4000–4009.

Rundlöf, T., C. Landersjö, K. Lycknert, A. Maliniak, and G. Widmalm. 1998. NMR investigation of oligosaccharide conformation using dipolar couplings in an aqueous dilute liquid crystalline medium. *Magn. Reson. Chem.* 36:773–776.

Sackmann, E. 1995. Physical basis of self-organization and function of membranes: physics of vesicles. *In* Handbook of Biological Physics. R. Lipowsky and E. Sackmann, editors. Elsevier Science, Amsterdam. 213–304.

Sano, Y., T. Sasaki, K. Kajiwara, H. Urakawa, H. Inoue, and Y. Hiragi. 1991. Mechanism of microgel formation of cellooligosaccharides by small-angle X-ray scattering method. *Photon Factory Activity Rep*. 9:196.

Saxena, K., P. Zimmermann, R. R. Schmidt, and G. G. Shipley. 2000. Bilayer properties of totally synthetic C16:0-lactosyl-ceramide. *Biophys. J.* 78:306–312.

Schneider, M. F., G. Mathe, M. Tanaka, C. Gege, and R. R. Schmidt. 2001. Thermodynamic properties and swelling behavior of glycolipid monolayers at interfaces. *J. Phys. Chem. B.* 105:5178–5185.

Seddon, J. M., G. Cevc, R. D. Kaye, and D. Marsh. 1984. X-ray diffraction study of the polymorphism of hydrated diacyl- and dialkylphosphatidylethanolamines. *Biochemistry*. 23:2634–2644.

Sen, A., A. P. Brain, P. J. Quinn, and W. P. Williams. 1982. Formation of inverted lipid micelles in aqueous dispersions of mixed sn-3-galactosyldiacylglycerols induced by heat and ethylene glycol. *Biochim. Biophys. Acta.* 686:215–224.

Shipley, G. G., J. P. Green, and B. W. Nichols. 1973. The phase behavior of monogalactosyl, digalactosyl, and sulphoquinovosyl diglycerides. *Biochim. Biophys. Acta.* 311:531–544.

Springer, T. A. 1995. Traffic signals on endothelium for lymphocyte recirculation and leukocyte emigration. *Annu. Rev. Physiol.* 57:827–872.

Tamada, K., H. Minamikawa, M. Hato, and K. Miyano. 1996. Phase transition in glycolipid monolayers induced by attractions between oligosaccharide head groups. *Langmuir*. 12:1666–1674.

Varki, A. 1994. Selectin ligands. *Proc. Natl. Acad. Sci. USA*. 91:7390–7397.

Vogel, J., G. Bendas, U. Bakowsky, G. Hummel, R. R. Schmidt, U. Kettmann, and U. Rothe. 1998. The role of glycolipids in mediating cell adhesion: a flow chamber study. *Biochim. Biophys. Acta*. 1372:205–215.

Warren, B. E. 1969. X-ray Diffraction. Addison-Wesley, Reading, MA.

Wiener, M. C., R. M. Suter, and J. F. Nagle. 1989. Structure of the fully hydrated gel phase of dipalmitoylphosphatidylcholine. *Biophys. J.* 55:315–325.